



ISSN: 0067-2904

## Synthesis, Characterization, Thermal Studies, and Antioxidant Activities of Azo Dye[2-[(3-Hydroxyphenyl)diazinyl]-1,2-Benzothiazol-3(2H)-one-1,1-Dioxide]and Metal Ion Complexes

Fatimah Al-zahraa SH. H. , Abbas Ali Salih Al-Hamdani

Department of Chemistry, College of Science for Women, University of Baghdad, Iraq

Received: 11/9/2023 Accepted: 9/12/2023 Published: xx

### Abstract

The new azo dye was synthesized *via* the reaction of the diazonium salt form of 3-aminophenol with 2-hydroxyquinoline. This dye was then used to access a series of complexes with the chlorides of manganese, iron, zinc, cadmium, and vanadium sulfate. The prepared ligand and its complexes were characterized by FT-IR spectroscopy, UV-visible spectroscopy, mass spectrometry, thermogravimetric analysis, differential scanning calorimeter, and microelemental analysis. Conductivity, magnetic susceptibility, metal content, and chlorine content of the complexes were also measured. The ligand and cadmium complex were identified using  $^1\text{H}$  NMR and  $^{13}\text{C}$  NMR spectroscopy. The results showed that the shape of the ligand is a trigonal planar, and the complex shapes are tetrahedral, except for vanadium, which is a square-based pyramid. Additionally, the findings demonstrated that the complexes include water inside the coordination field and that each and every one of them is a non-electrolyte. The dye used the complexes prepared from it to determine their ability to inhibit free radicals by measuring their ability as antioxidants using DPPH as a free radical. D-ascorbic acid was employed as a standard substance in determining the value of  $\text{IC}_{50}$ , as it was found that the ligand had a high ability to inhibit free radicals. The ability to inhibit the complexes varied according to the value of  $\text{IC}_{50}$ , and the results are as follows:  $\text{H}_2\text{L} > \text{D-ascorbic acid} > \text{Zn-complex} > \text{Fe-complex} > \text{V-complex} > \text{Cd-complex} > \text{Mn-complex}$ .

**Keywords:** 3-Aminophenol, Antioxidant, Azodye complexes, 2-Hydroxyquinoline, Thermodynamic parameter.

تحضير، تشخيص، دراسة التحلل الحراري وانشطة مضادات الاكسدة لصبغة ازو (2-3-هايدروكسي فنيل دايانيل)-1,2-بنزو ثيازول-3-اون 1,1-ثنائي اوكسايد) مع معقدات ايونات الفلزات

فاطمة الزهراء شاكر حاتم و عباس علي صالح الحمдاني

قسم الكيمياء، كلية العلوم للبنات، جامعة بغداد، بغداد، العراق

### الخلاصة

حضرت صبغة الازو الجديدة من تفاعل ملح الديازونيوم من 3-امينو فينول مع 2-هايدروكسي كوينولين استخدمت الصبغة لتحضير سلسلة من المعقدات مع كلوريدات كل من المنغنيز والحديد والخرصين والكاميوم وكبريتات الفناديوم، شخص الليكاند والمعقدات المحضرة بطيف الاشعة تحت الحمراء وطيف الاشعة فوق البنفسجة-المرئية وطيف الكتلة والتحليل الحرارية الوزنية والمسعر التفاضلي والتحليل الدقيق للعناصر. وقياس

التوصيلية والحساسية المغناطيسية ومحتوى الفلز ومحتوى الكلور للمعقدات. تم التحقق من الليكاند ومعقد الكاديوم بطيف الرنين النووي المغناطيسي للبروتون والكربون. أظهرت النتائج ان الليكاند ثلاثي السن والمعقدات رباعية السطوح عدا الفناديوم كان هرم مربع القاعدة. فضلاً عن احتواء المعقدات على الماء داخل مجال التناسق وان جميعها غير الكتروليتية. استخدم الصبغة المعقدات المحضرة منها لتحديد قابليتها على كبح الجذور الحرة من خلال قياس قابليتها كمضادات اكسدة باستخدام مادة DPPH كجذر حر وحامض الاسكوريك كمادة قياسية وتحديد قيمة  $IC_{50}$  حيث وجد ان الليكاند يمتلك قابلية عالية على كبح الجذور الحرة والمعقدات تفاوتت قابليتها على الكبح حسب قيمة  $IC_{50}$  وكانت النتائج كما يلي:

( $H_2L > Ascorbic\ acid > Zn-complex > Fe-complex > V-complex > Cd-complex > Mn-complex$ )

**الكلمات المفتاحية:** مضادات الاكسدة, 3-امينو فينول , معقدات اصباغ الازو, الثوابت الترموديناميكية و-2-هيدروكسيكوينولين.

## 1. Introduction

Azo dyes are among the most widely used, useful, and important types of chemical compounds, with diverse applications in science and technology[1-2]. The presence of an azo moiety (-N=N-) coupled with two monocyclic or polycyclic moieties identifies azo compounds[3]. Aromatic or heterogeneous systems are either unique or homologous[4]. Because of their distinctive physical and chemical characteristics and biological activities, they have a broad variety of uses in the pharmaceutical, cosmetic, food, dyeing, and textile industries [5]. However, their coloring job remains their most popular and favorite tool. The medicinal significance of azo compounds is widely recognized for their antibacterial, antifungal, and anti-HIV properties [6]. The majority of azo dyes are used to color textiles, and it is estimated that 10% of the dyes used in these dyeing procedures are not. They stick to the fibers and end up in wastewater treatment[7]. Some azo dyes are carcinogenic, and this is due to degradation products such as benzidine, which activate various tumors in humans and animals. Aromatic amines found in many azo dyes affect human health, cause allergic reactions, and cause other diseases. Different metal quinoline complexes have been shown to be more effective than the parent quinoline because of their interesting bioactivity. Many studies have been performed on heterocyclic azo dyes and their metal chelators. Dyed azo metal chelates are of interest for use in molecular memory storage, nonlinear visualizations, and printing systems[8-10]. This research aims to prepare novel complexes of the metal ions ( $Cd^{+2}$ ,  $Zn^{+2}$ ,  $Fe^{+3}$ ,  $Mn^{+2}$ , and  $V^{+4}$ ) using the azo ligand  $H_2L$ . Thereafter, characterization by spectroscopic analysis, thermal stability, and thermal decomposition will be studied using DSC and TGA curves, and the antioxidant activity of these compounds will be assessed against the DPPH radical and compared with D-ascorbic acid as a reference.

## 2. Experimental

### 2.1. Material and Methods

All the materials used in this work were provided by SigmaAldrich, Merck, and other companies. The Urovector model EA/3000 singleV30 analyzer was used to record elemental microanalyses for carbon, hydrogen, nitrogen, and sulfur (C.H.N.S.). Through a gravimetric approach, mineral ions were identified as M-O. Using DMSO as a solvent, a conductometer W-T-W estimated molar conductivities ( $1 \times 10^{-3}$  M) at 25 °C. Mass spectrometry data were recorded using a Q-P-50-A-D-I Analysis Shimadzu QP(E170Ev)-2010-Pluss spectrometer. The UV-1800 Shimadzu Spectrophotometer was used to record the UV-visible absorption. The  $^1H$  and  $^{13}C$ NMR spectra were measured using a Bruker (400MHz) spectrometer. The Fourier Transform Infrared (FT-IR) spectra were recorded using an IR Prestige-21, and the instruments

employed were the Braker 4000-500  $\text{cm}^{-1}$  and the Shimadzu 4000-200  $\text{cm}^{-1}$ . Metals were identified using a Shimadzu (F.A.A.) 680 G atomic clock. Magnetic properties were used with the balancing susceptibility model MSR-MKI. All earlier types of thermal analysis employed Perkin-Elmer Pyris Diamond DSC/TGA.

### 2.2. Synthesis of azo dye ligand: [2-[(3-hydroxyphenyl)diazenyl]-1,2-benzothiazol-3(2H)-one 1,1-dioxide]

To a solution of 3-aminophenol (1g, 0.008mmol) in HCl (2 mL, xx N), ethanol (15mL), and distilled water (10 mL) at 0 to 5 °C, a solution of NaNO<sub>2</sub> (1 g, 14.49mmol) in H<sub>2</sub>O (10 mL) was added gradually. The reaction mixture was stirred for 45 minutes before adding a solution of 2-hydroxyquinoline (1.16 g, 0.008 mmol) in ethanol (15 mL). A change to a dark-colored solution was observed after 30 minutes of stirring. The solid crude material formed was filtered and dried to give a brown precipitate with an 87% yield that melts at 253-255 °C.

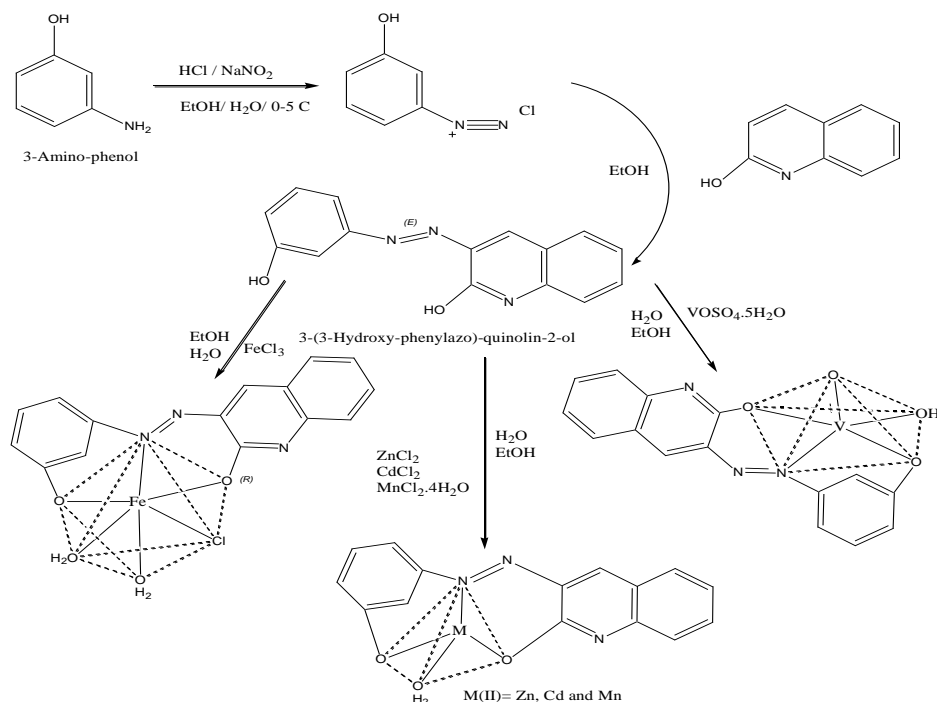
### 2.3. General approach for metal complexes synthesis

A solution of metal salt [VOSO<sub>4</sub>·5H<sub>2</sub>O (0.1 g, 1 mmol), FeCl<sub>3</sub> (0.058g, 1 mmol), MnCl<sub>2</sub>·4H<sub>2</sub>O (0.08g, 1 mmol), ZnCl<sub>2</sub> (0.05g, 1 mmol), or CdCl<sub>2</sub> (0.07g, 1 mmol)] in water (10 mL). Azo ligand H<sub>2</sub>L (0.1g, 1mmol) was added drop by drop to the solution before heating at 40 °C for 2 hours. By briefly submerging the solid complexes in hot ethanol, any unreacted components were separated from them and eliminated. The complexes were gathered, dried, and weighed.

## 3. Results and discussion

### 3.1. Physical and analytical data for the ligand (H<sub>2</sub>L) and the complexes synthesized

The reaction of metal salts and ligand afforded the desired complexes as shown in Scheme 1. The findings of the elemental analysis show that all compounds have a 1:1 ratio of M:L. The results of the microelemental analysis were consistent with the theoretical calculations, as shown in Table 1.



**Scheme 1-** Formation for ligand (H<sub>2</sub>L) and their metal complexes

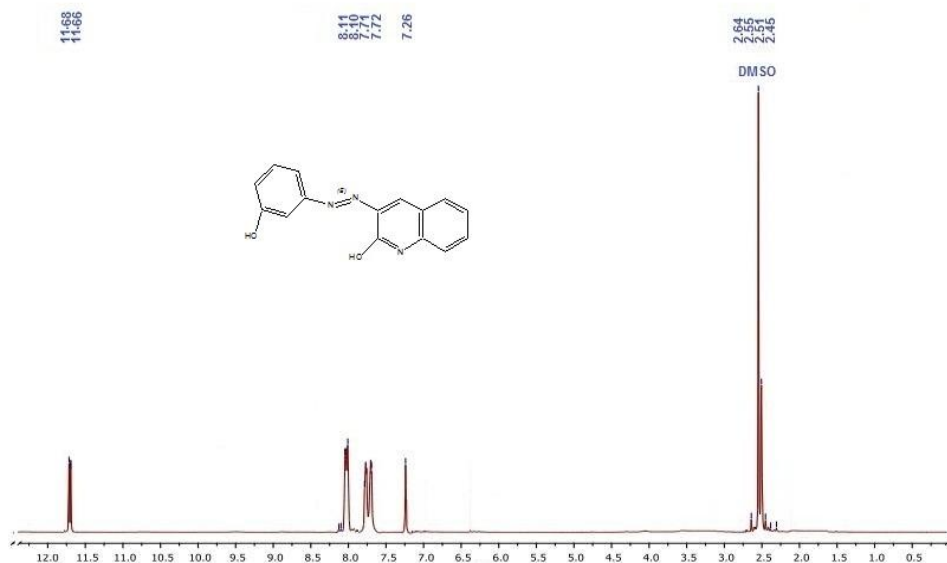
**Table 1:** Some elemental physical characteristics investigations of ligand and complexes

Compound no.	Formula Molecular weight	m.p.(°C)	Ratio	C (%)	H (%)	N (%)	M (%)	Cl (%)	Conductivity In DMSO cm <sup>2</sup> Ω <sup>-1</sup> mol <sup>-1</sup>
1	C <sub>15</sub> H <sub>11</sub> N <sub>3</sub> O <sub>2</sub> 265.27	253-255	found	67.92	4.18	15.84		-	
			Calculated	67.09	3.72	16.81			
2	C <sub>15</sub> H <sub>11</sub> N <sub>3</sub> O <sub>4</sub> V 348.21	289-291	found	51.74	3.18	12.07	14.63	-	12
			Calculated	50.62	3.83	12.28	14.88		
3	C <sub>15</sub> H <sub>11</sub> N <sub>3</sub> O <sub>3</sub> Mn 336.20	276-278	found	53.59	3.35	12.50	16.34	-	16
			Calculated	52.69	3.09	13.16	13.02		
4	C <sub>15</sub> H <sub>13</sub> N <sub>3</sub> O <sub>4</sub> ClFe 390.58	292-294	found	46.13	3.35	10.76	14.30	9.08	19
			Calculated	46.89	3.97	11.89	13.54	9.57	
5	C <sub>15</sub> H <sub>11</sub> N <sub>3</sub> O <sub>3</sub> Zn 346.66	277-280	found	51.97	3.20	12.12	18.86	-	11
			Calculated	50.99	4.11	13.10	18.55		
6	C <sub>15</sub> H <sub>11</sub> N <sub>3</sub> O <sub>3</sub> Cd 393.68	296-299	found	45.76	2.82	10.67	28.55	-	10
			Calculated	44.89	3.55	11.89	28.22		

### 3.2. <sup>1</sup>H NMR and <sup>13</sup>C NMR data of the azo ligand and Cd complex

The <sup>1</sup>H NMR and <sup>13</sup>C NMR spectra of azo ligand are displayed in Figure 1. The <sup>1</sup>H NMR data in DMSO-*d*<sub>6</sub> (ppm) are 2.45 (2H, s, N-H), 7.26 (1H, s, Ar-H), 7.72-7.71 (1H, d, Ar-H), 11.68-11.66 (1H, s, 2OH) [11]. <sup>13</sup>C NMR data in DMSO-*d*<sub>6</sub> (ppm) are 127.5 (C1), 149.0 (C2), 118.2 (C3), 145.0 (C4), 157.2 (C5), 169.8 (C6), 132.2 (C7), 165.3 (C8), 137.3 (C9), 166.9 (C10), 155.2 (C11), 122.2 (C12), 178.1 (C13), 182.0 (C14), 189.75 (C15) [12].

The <sup>1</sup>H NMR and <sup>13</sup>C NMR spectra of Cd-complex are displayed in Figure 2. The <sup>1</sup>H NMR data of Cd complex in DMSO-*d*<sub>6</sub> (ppm) are 3.34 (DHO impurities), 8.46-7.36 (9H, m, Ar-H). <sup>13</sup>C NMR data in DMSO-*d*<sub>6</sub> (ppm) are 106.6 (C1), 189.8 (C2), 145.5 (C3), 181.7 (C4), 190.2 (C5), 118.6 (C6), 137.6 (C7), 127.8 (C8), 132.5 (C9), 155.4 (C10), 172.6 (C11), 158.0 (C12), 178.7 (C13), 165.8 (C14), 196.2 (C15) [11].



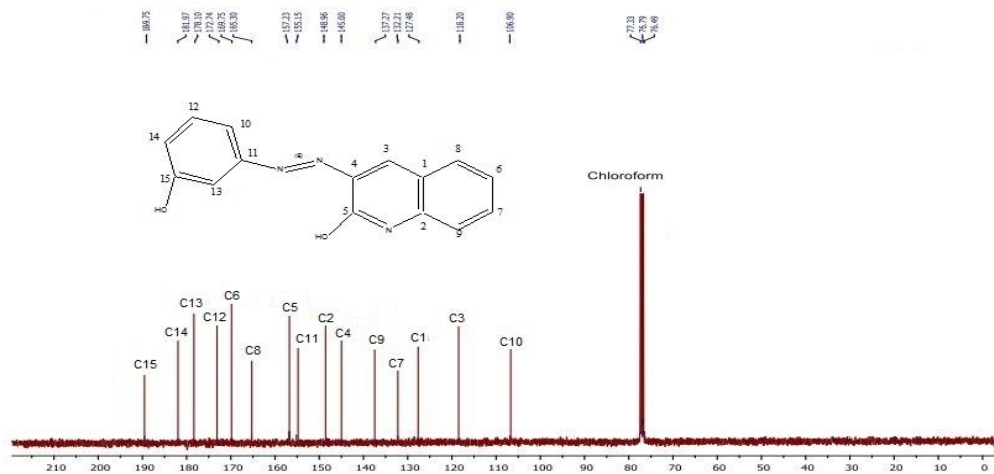


Figure 1 : <sup>1</sup>H NMR and <sup>13</sup>C NMR spectra of azo ligand (H<sub>2</sub>L)

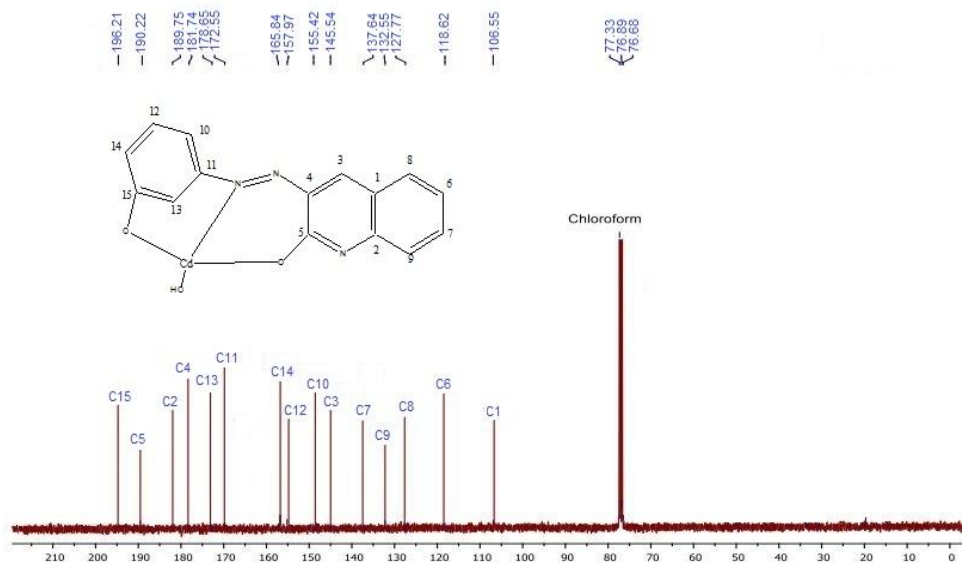
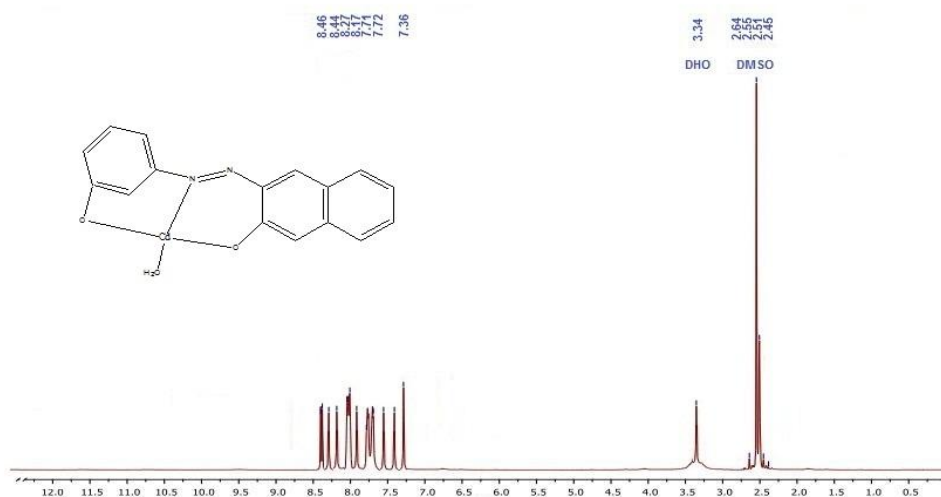
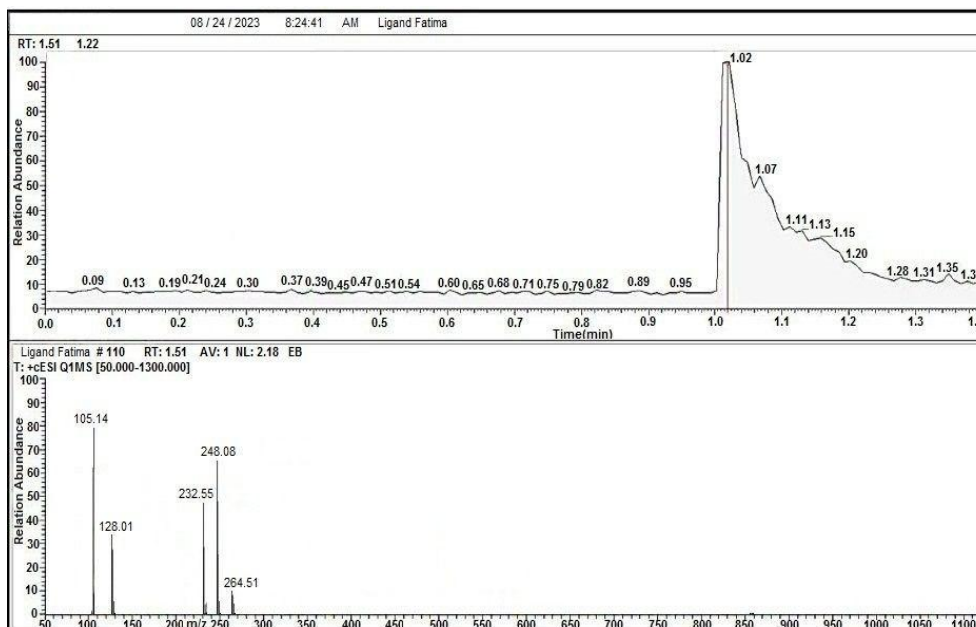


Figure 2: <sup>1</sup>H NMR and <sup>13</sup>C NMR spectra of the Cd complex

### 3.3. LC-mass spectra for ligand and its complexes

One of the most crucial methods for characterizing the ligand ( $H_2L$ ) and some products is LC-Mass spectrum testing. This method is supplementary to the other methods that estimate the molecular weight of the chemical using the relationship  $(m/z)$ [13]. The fragmentation pattern and the extract mass for each pattern are shown in Scheme 2. The fragment's molecular ion peak  $[M]^+$  of  $C_{15}H_{10}N_3O^+$  is easily visible, and its relative abundance is about 67% in Figure 3. Other peaks observed at 45, 32, and 88% belong to the  $C_{15}H_{10}N_3^+$ ,  $C_9H_6N^+$ , and  $C_6H_5N_2^+$  ions, respectively[8]. For the  $[Cd(L)H_2O]$  (Figure 4 and Scheme 2), we can observe the molecular ion peak ( $M^+$ ) at 392.33m/z with a relative abundance of 10%, and the next patterns are  $C_{15}H_7CdN_3O_2^{++}$ ,  $C_{15}H_8CdN_3O^+$ ,  $C_{15}H_8CdN_2O^{++}$ ,  $C_9H_4CdN_2O^{++}$  and  $C_6H_5^+$ , which correspond to 374.58 m/z, 358.78 m/z, 344.64 m/z, 267.69m/z, and 77.84m/z, respectively. In the  $[Mn(L)H_2O]$  complex (Scheme 2), the fragments ( $M^+$ ) at 336.42m/z with a relative abundance of 10%, and the next patterns are  $C_{15}H_8N_3O_2Mn^+$ ,  $C_9H_4N_3OMn^+$ ,  $C_9H_4N_2OMn^+$ ,  $C_9H_4NOMn^+$  and  $C_6H_4O^+$ , which corresponded to 317.42m/z, 255.02 m/z, 211.35m/z, 197.42m/z, and 92.33m/z. For  $[Fe(L)(H_2O)_2Cl]$  complex (Scheme 5), the fragments ( $M^+$ ) at 390.44m/z with a relative abundance of 15% and the next patterns are  $C_{15}H_9ClFeN_3O_2^+$ ,  $C_{15}H_9FeN_3O_2^+$ ,  $C_{15}H_9FeN_3O^+$ ,  $C_9H_5FeNO^+$ ,  $C_6H_5N_2^+$ ,  $C_7H_5N_2^{++}$  and  $C_2HFeO^+$  corresponded to 354.64m/z, 319.08 m/z, 303.32m/z, 198.14 m/z, 105.44 m/z, 103.21m/z, and 96.89m/z. In the  $[VO(L)H_2O]$  complex (Scheme 2), the fragments ( $M^+$ ) at 348.34m/z with relative abundance 20% and next pattern:  $C_{15}H_8N_3O_3V^+$ ,  $C_9H_4N_3O_2V^+$ ,  $C_9H_4N_2O_2V^+$ ,  $C_9H_4NO_2V^{++}$  and  $C_6H_4O^+$ , which corresponded to 329.22m/z, 237.01m/z, 223.22 m/z, 209.41m/z, and 92.36m/z. For the  $[Zn(L)H_2O]$  complex in Scheme 2, the next fragments ( $M^+$ ) are at 345.86m/z with a relative abundance of 25% and the next patterns are  $C_{15}H_8N_3O_2Zn^+$ ,  $C_{15}H_8ZnN_3O^+$ ,  $C_{15}H_8ZnN_2O^{++}$ ,  $C_9H_3ZnN_2O^{++}$  and  $C_6H_5^+$  which correspond to 327.63m/z, 311.65 m/z, 297.35m/z, and 220.54m/z, respectively[14].



**Figure 3:** Mass spectrum of ligand  $H_2L$

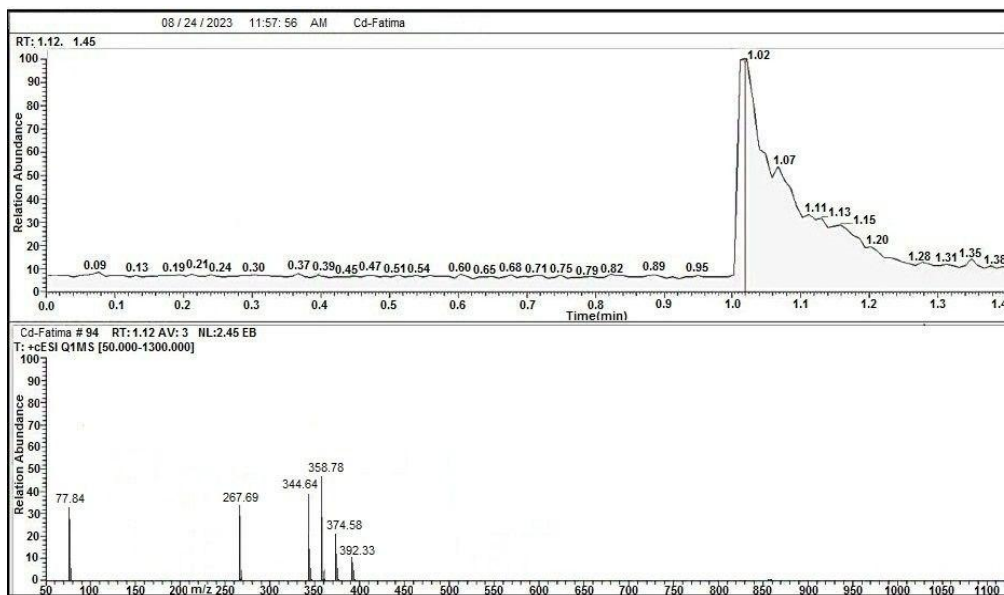
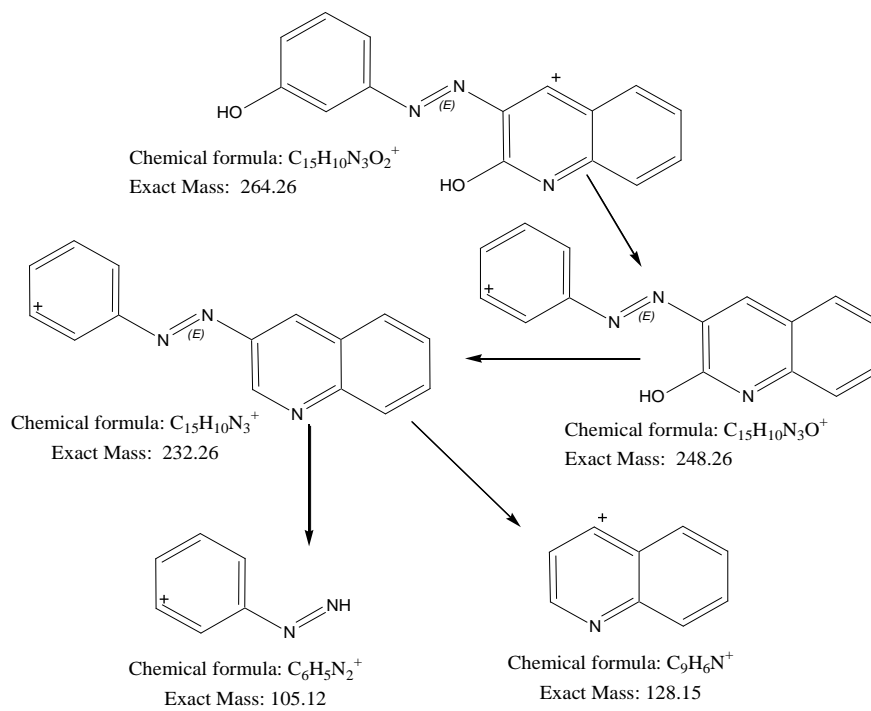
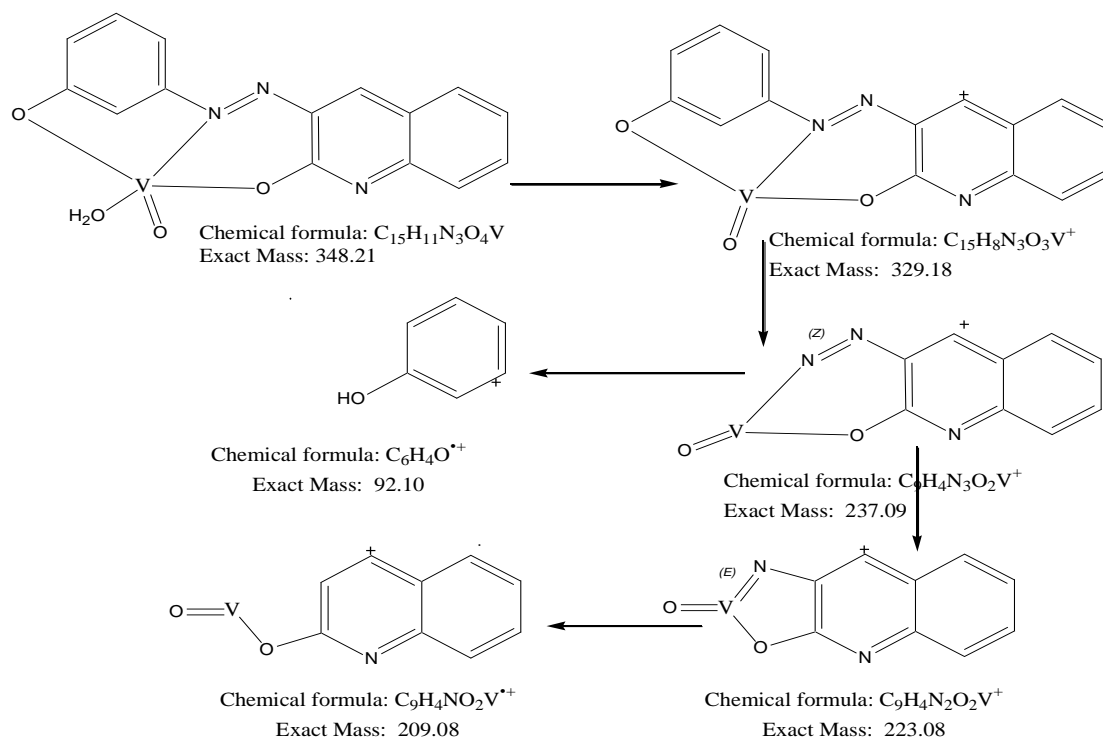
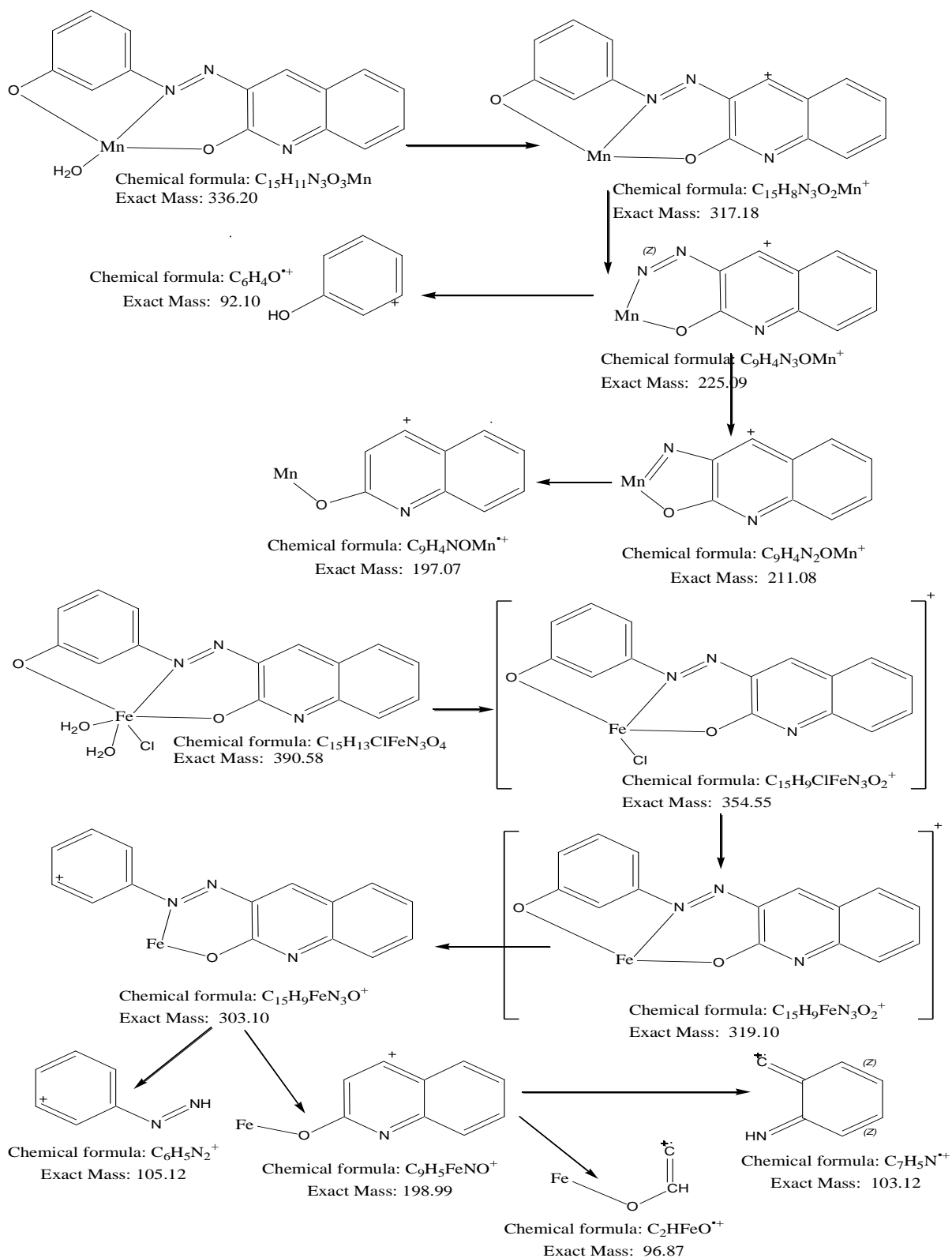


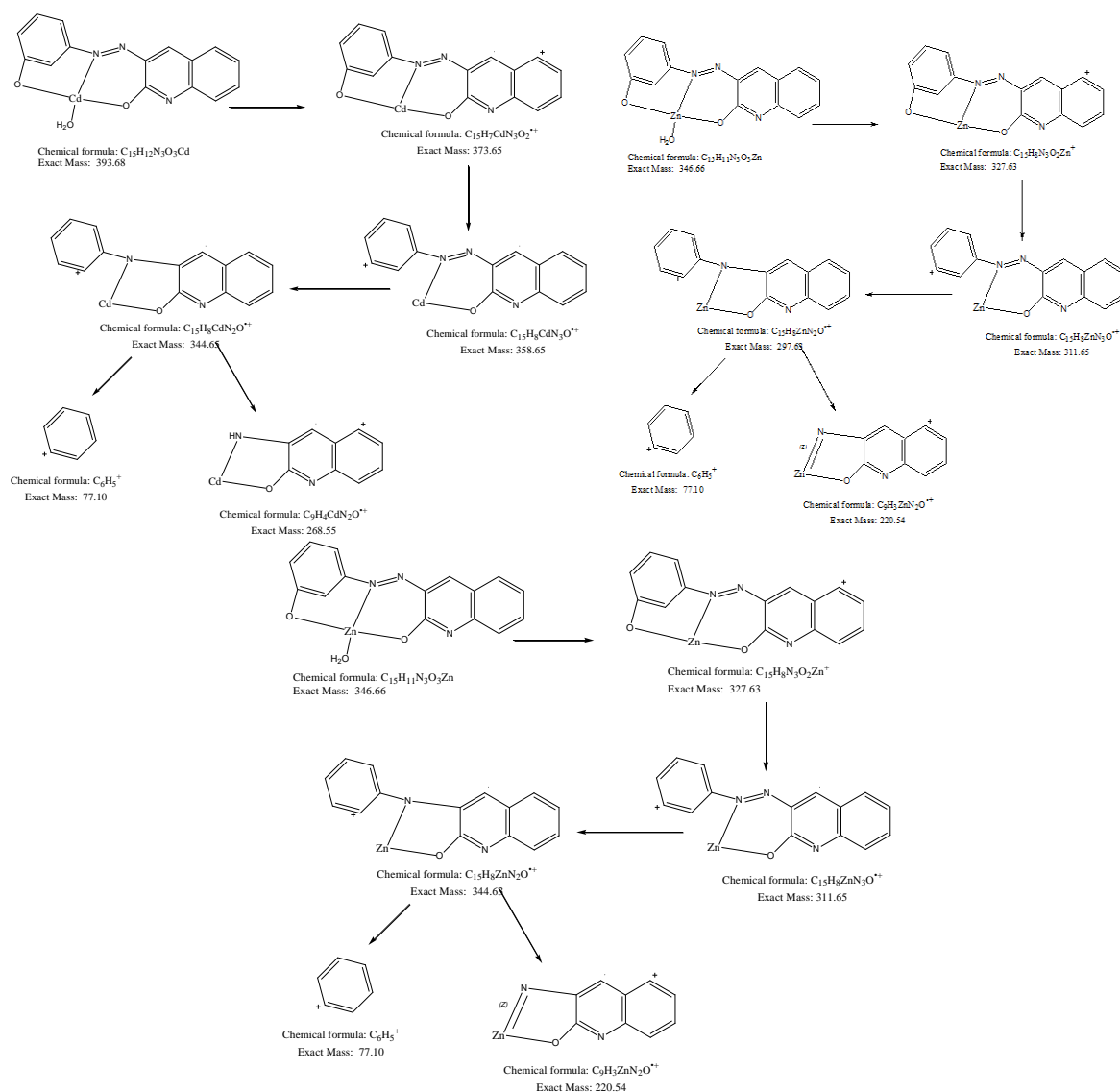
Figure 4: Mass spectrum of Cdcomplex











**Scheme 2:** Pattern of fragmentation of ligand and their complexes

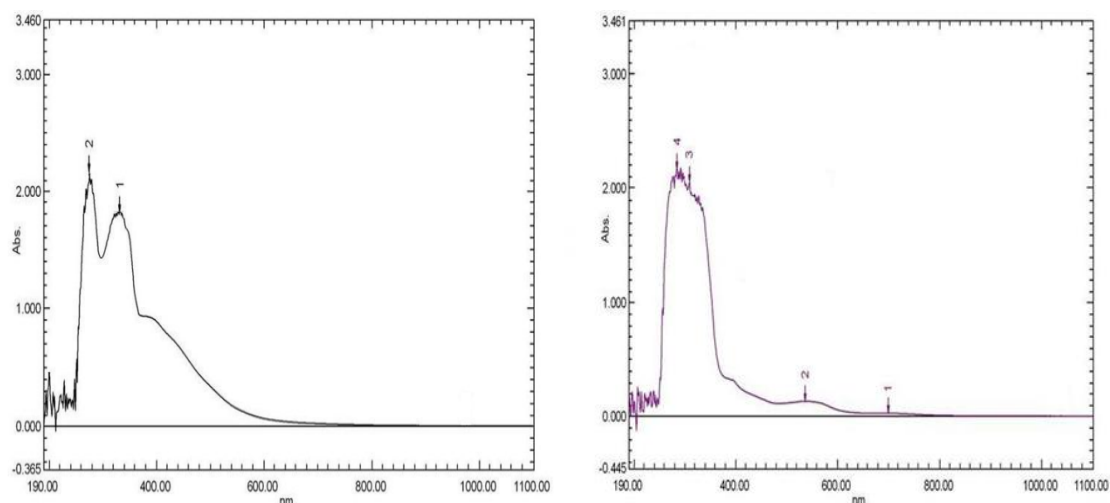
### 3.4. The ligand ( $H_2L$ ) and its complexes are studied by UV-Vis

The electronic spectrum for ligand ( $H_2L$ ) in Figure 5 exhibits strong absorptions at 275 nm and  $36363.64\text{cm}^{-1}$  ascribed to the  $\pi \rightarrow \pi^*$  transition and a peak at 350 nm and  $28571.43\text{cm}^{-1}$  attributed to the  $n \rightarrow \pi^*$  transition, a peak with a high intensity band formed with absorption maxima [15]. The electronic transition of the  $V^{+4}$  complex depicts peaks of 280, 345, 390, 620, and 780 nm assigned to  $\pi \rightarrow \pi^*$ ,  $n \rightarrow \pi^*$ ,  ${}^2B_{2g} \rightarrow {}^2E_g$ , and  ${}^2B_{2g} \rightarrow {}^2B_{1g}$ , respectively, which is indicative of a square pyramidal geometry. The electronic spectrum of the divalent zinc compound was studied, and it was found that it does not give d-d transitions because it contains ( $d^{10}$ ) in the valence shell. However, it gave two peaks, each belonging to the ligand spectrum: peaks at 290 nm and 470 nm assigned to  $\pi \rightarrow \pi^*$  and  $n \rightarrow \pi^*$ , respectively, which is indicative of a tetrahedral. The electronic spectrum of the  $Cd^{+2}$  compound was studied, and it was found that it does not give d-d transitions because it contains ( $d^{10}$ ) in the valence shell, but it gave three peaks, each belonging to the ligand spectrum, peaks in 255, 340, and 390 nm assigned to  $\pi \rightarrow \pi^*$ ,  $n \rightarrow \pi^*$ , and C.T.  $M \rightarrow L$ , respectively, which is indicative of a tetrahedral. The electronic absorption of  $Mn^{2+}$  complex exhibited peaks of 235, 295, 325, 595, and 785 nm ascribed to the  $\pi \rightarrow \pi^*$ ,  $n \rightarrow \pi^*$ , C.T.  $M \rightarrow L$ ,  ${}^6A_{1g} \rightarrow {}^4E_{g(G)}$ ,  ${}^6A_{1g} \rightarrow {}^4T_{2g(G)}$ ,  ${}^6A_{1g} \rightarrow {}^4T_{1g(G)}$ , and  ${}^6A_{1g} \rightarrow {}^4T_{2g(D)}$ , respectively, which is indicative of a tetrahedral. The electronic transition of  $Fe^{+3}$  complex show in Figure 6 exhibited peaks of 270, 310, 545, and 720 nm assigned to  $\pi \rightarrow \pi^*$ ,  $n \rightarrow \pi^*$ , C.T.  $M \rightarrow L$ ,

${}^6A_{1g} \rightarrow {}^4T_{2g}(G)$ ,  ${}^6A_{1g} \rightarrow {}^4T_{1g}(G)$ , and  ${}^6A_{1g} \rightarrow {}^4E_g(D)$ , respectively, which is indicative of an octahedral geometry. Table 2 displays the electronic assignment of metal complexes [16,17]. All complexes are non-electrolytes.

**Table 2:** The ligand (H<sub>2</sub>L) and its complexes are studied by UV-Vis

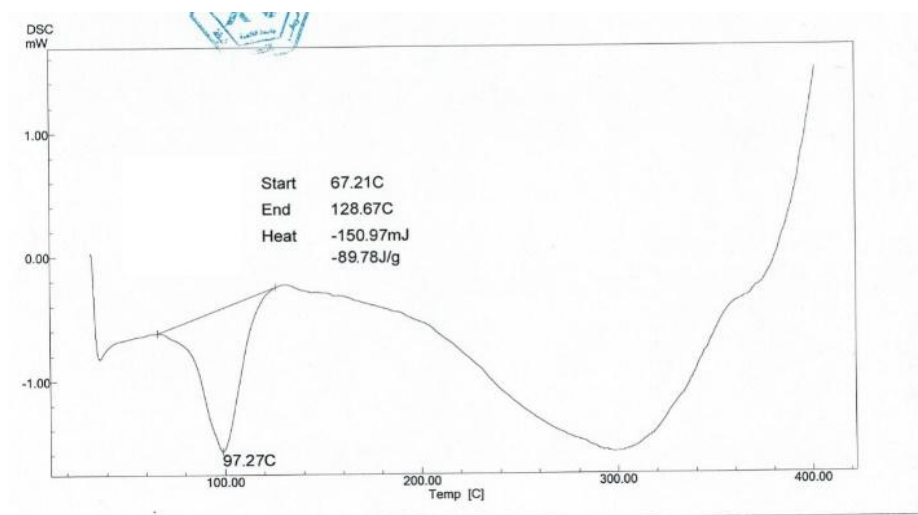
Compound	$\lambda$ nm	$\nu$ cm <sup>-1</sup>	Abs	$\epsilon_{max}$ Lmol <sup>-1</sup> cm <sup>-1</sup>	Assignment	$\mu_{eff}$ (B.M) found (calculate)	Hybridization	Distribution
Ligand H <sub>2</sub> L	275 350	36363.6 4 28571.4 3	1.89 2.13	1890 2130	$\pi \rightarrow \pi^*$ $n \rightarrow \pi^*$			
[VO(L)H <sub>2</sub> O] Square pyramidal	280 345 390 620 780	35714.2 9 28985.5 1 25641.0 3 16129.0 3 12820.5 1	1.20 0 1.12 0 0.40 0 0.26 0 0.25 0	1200 1120 400 260 250	$\pi \rightarrow \pi^*$ $n \rightarrow \pi^*$ C.T ${}^2B_{2g} \rightarrow {}^2E_g$ ${}^2B_{2g} \rightarrow {}^2B_{1g}$	1.81 (1.73)	dsp <sup>3</sup>	t <sub>2g</sub> <sup>1</sup> e <sub>g</sub> <sup>0</sup>
[Mn(L)H <sub>2</sub> O] Tetrahedral	235 295 325 595 785	42553.1 9 33898.3 1 30769.2 3 16806.7 2 12738.8 5	2.12 5 1.89 5 0.89 0 0.62 5 0.59 5	2125 1895 890 625 595	$\pi \rightarrow \pi^*$ $n \rightarrow \pi^*$ C.T M→L ${}^6A_{1g} \rightarrow {}^4E_g(G)$ ) ${}^6A_{1g} \rightarrow {}^4T_{2g}(G)$	5.44 (5.91)	SP <sup>3</sup>	e <sup>2</sup> t <sub>2</sub> <sup>3</sup>
[Fe(L)H <sub>2</sub> O Cl] Octahedral	270 310 545 720	37037.0 4 32258.0 6 18348.6 2 13888.8 9	2.11 5 1.99 8 0.25 0 0.12 5	2115 1998 250 125	$\pi \rightarrow \pi^*$ $n \rightarrow \pi^*$ ${}^6A_{1g} \rightarrow {}^4E_g(G)$ ) ${}^6A_{1g} \rightarrow {}^4T_{2g}(G)$	5.17 (5.91)	SP <sup>3</sup> d <sup>2</sup>	T <sub>2g</sub> <sup>3</sup> e <sub>g</sub> <sup>2</sup>
[Zn(L)H <sub>2</sub> O] Tetrahedral	290 470	34482.7 6 2127.66	2.31 5 0.52 5	2315 525	$\pi \rightarrow \pi^*$ $n \rightarrow \pi^*$	Diamagnetic (0)	SP <sup>3</sup>	e <sup>4</sup> t <sub>2</sub> <sup>6</sup>
[Cd(L)H <sub>2</sub> O] Tetrahedral	255 340 390	39215.6 9 29411.7 6 25641.0 3	2.12 0 1.98 0 0.89 0	2120 1980 890	$\pi \rightarrow \pi^*$ $n \rightarrow \pi^*$ C.T M→L	Diamagnetic (0)	SP <sup>3</sup>	e <sup>4</sup> t <sub>2</sub> <sup>6</sup>



**Figure 5** UV-Vis spectrum of ligand (H<sub>2</sub>L) **Figure6-** UV-Vis spectrum of Fe-complex

### 3.5. Thermal analysis

The results of the thermal analysis can be seen in Tables 4 and 5 and in Figures 7 and 8 for the ligand (H<sub>2</sub>L) and the complexes that were made [18]. Scheme 8 outlines the potential breakdown response of metal complexes. Based on the thermograms, computations of the decomposition phases, temperature ranges, decomposition products, and weight loss complex percentages indicated consistency. That verifies the elemental analysis findings and recommended equations between their thermal decomposition results and computed values[10]. In this work, it was noted that in the ligand and metal complexes of V<sup>+4</sup>, Fe<sup>+3</sup>, Zn<sup>+2</sup>, Cd<sup>+2</sup>, and Mn<sup>+2</sup>, the remaining ligand was carbon and the remaining metal oxide. Based on the results of the thermogravimetric studies, it can be shown that the complexes and the ligand form one to three distinct phases. Using the DCS curve, the thermodynamic parameters enthalpy  $\Delta H$ , entropy  $\Delta S$  and Gibbs free energy ( $\Delta G$ ) were calculated[19].



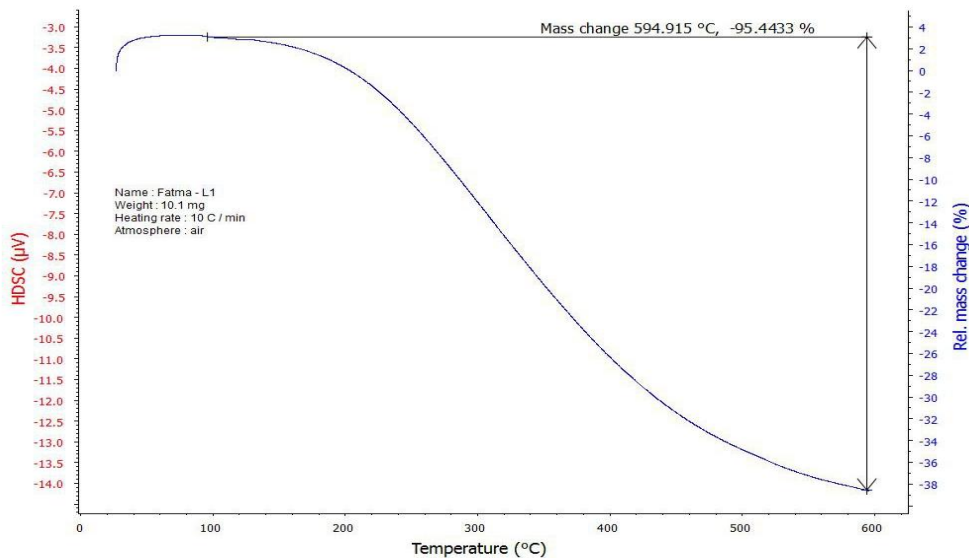


Figure 7: TGA&DSC curve of Ligand (H<sub>2</sub>L)

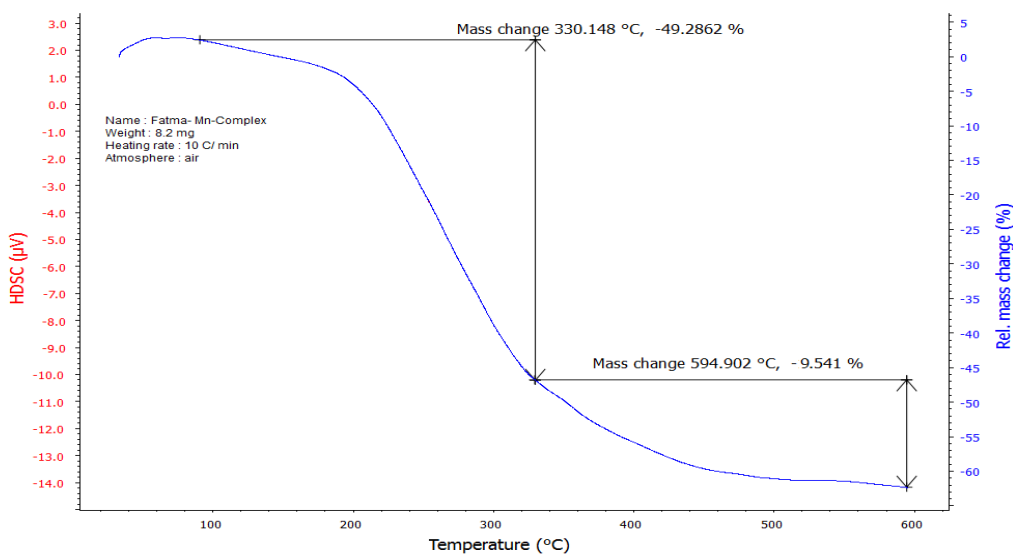
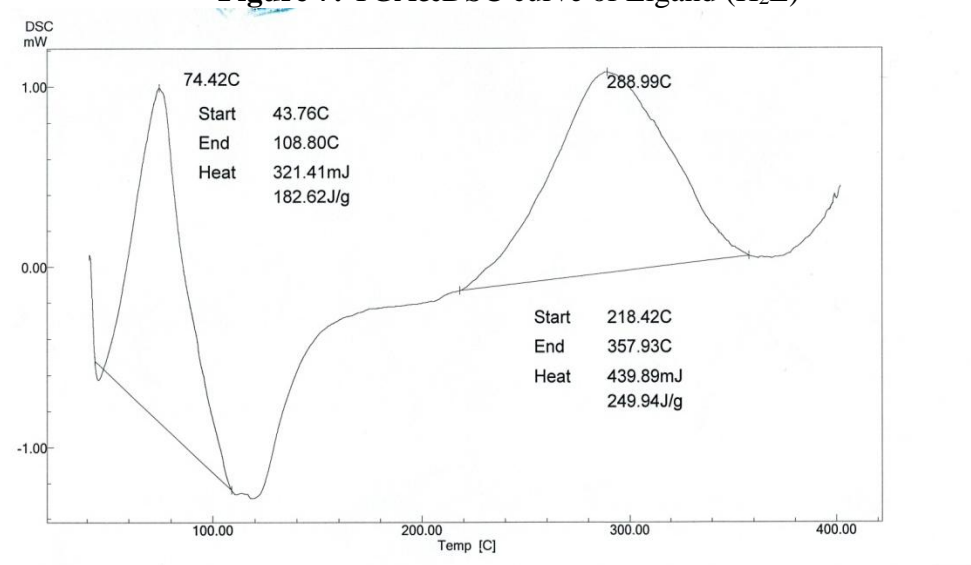
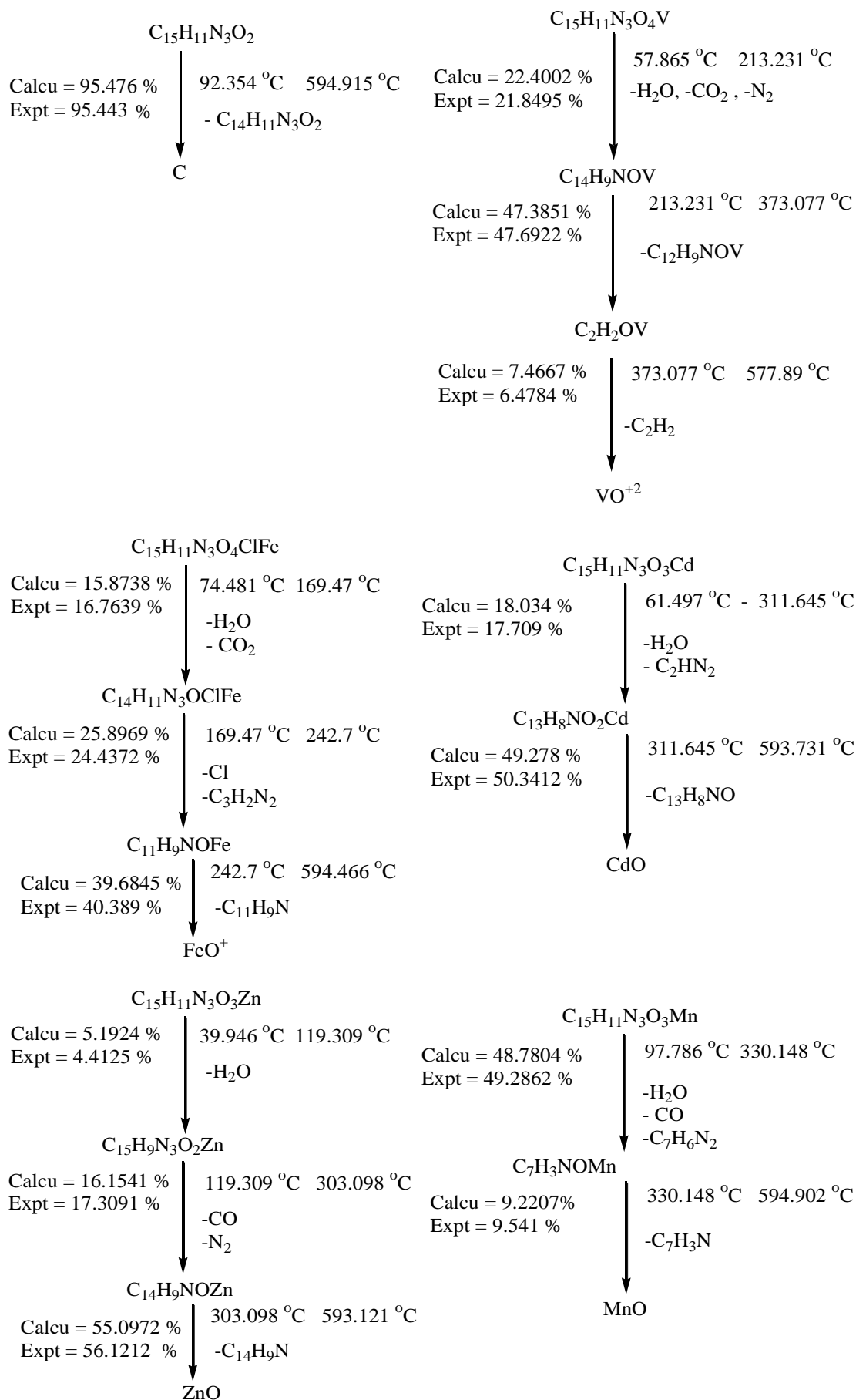


Figure 8: TGA&DSC curve of MnComplex



**Scheme 8:** Tentative decomposition reaction of ligand and metal complexes

**Table3:** Thermal decomposition DSC of Ligand and some complexes

Compound	T <sub>i</sub> /°C	T <sub>f</sub> /°C	Maximum temperature point (°C)	ΔH (J/g)	ΔS (J)	ΔG (J)	Type
H <sub>2</sub> L	67.21	128.67	97.27	-89.78	-1.4608	52.31	endothermic
[Fe(L)(H <sub>2</sub> O)Cl]	105.94	112.21	316.57	-1.19	-0.178	55.159	endothermic
	156.16	159.31		-0.79	-0.251	78.669	endothermic
	314.05	319.44		-2.78	-0.515	160.256	endothermic
[Zn(L)H <sub>2</sub> O]	263.32	276.00	257.72	-36.90	-2.910	713.065	endothermic
	278.01	287.47	270.71	-11.55	-1.220	331.379	endothermic
			281.09				
[Mn(L)H <sub>2</sub> O]	43.76	108.80	74.42	182.62	2.807	49.512	endothermic
	218.42	357.93	288.99	249.94	1.791	-267.641	exothermic
[Cd(L)H <sub>2</sub> O]	387.65	395.13	392.40	-3.03	-0.405	155.892	endothermic
[VO(L)H <sub>2</sub> O]	46.17	63.49	56.51	-1.63	-0.094	5.2179	endothermic
	60.34	98.63	76.54	-24.35	-0.635	24.252	endothermic
	172.41	257.74	223.54	54.84	0.642	-88.673	exothermic
	324.45	334.99	332.57	-1.75	-0.166	53.456	endothermic

**Table 4:** TGA data of the ligand H<sub>2</sub>Landsome complexes

Compound	Step	T <sub>i</sub> /°C	T <sub>f</sub> /°C	Weight mass loss%		Reaction
				Calc	Found	
Ligand	1	92.354°C	594.915°C	95.476%	95.443%	-C <sub>14</sub> H <sub>11</sub> N <sub>3</sub> O <sub>2</sub>
						C
Calculated: 95.476% , Final= 4.524%, Estimated95.443% Final=4.557%						
Cd-complex	1	61.497°C	311.645°C	18.034%	17.709%	-H <sub>2</sub> O-C <sub>2</sub> HN <sub>2</sub>
						-C <sub>13</sub> H <sub>8</sub> NO
	2	311.645°C	593.731°C	49.278%	50.3412%	CdO
Calculated: 67.312% Final= 32.688% Estimated 68.0502% Final 31.9498%						
Mn-complex	1	97.786°C	330.148°C	48.7804%	49.2862%	-H <sub>2</sub> O, -CO
						-C <sub>7</sub> H <sub>6</sub> N <sub>2</sub>
	2	330.148°C	594.902°C	9.2207%	9.541%	-C <sub>7</sub> H <sub>3</sub> N
						MnO
Calculated:58.0011% Final 41.9989% Estimated 58.8272% Final=41.1728%						
V-complex	1	57.865°C	213.231°C	22.4002%	21.8495%	-H <sub>2</sub> O-CO <sub>2</sub>
						-N <sub>2</sub>
						-C <sub>12</sub> H <sub>9</sub> NO
	2	213.231°C	373.077°C	47.3851%	47.6922%	
	3	373.077°C	577.89°C	7.4667%	6.4784%	-C <sub>2</sub> H <sub>2</sub>
						VO <sup>+2</sup>
Calculated: 77.252% Final= 22.748% Estimated 71.8796% Final=28.1204% 28.1204%						
Fe-complex	1	74.481°C	169.47°C	15.8738%	16.7639%	-H <sub>2</sub> O-CO <sub>2</sub>
						-Cl, -C <sub>3</sub> H <sub>2</sub> N <sub>2</sub>
						-C <sub>11</sub> H <sub>9</sub> N
	2	16.47°C	242.7°C	25.8969%	24.4372%	
	3	242.7°C	594.466°C	39.6845%	40.389%	FeO <sup>+</sup>
Calculated: 81.4552% Final= 18.5448% Estimated 81.5901% Final=18.4099%						
Zn-complex	1	39.946°C	119.309°C	5.1924%	4.4125%	-H <sub>2</sub> O
						-CO -N <sub>2</sub>
						-C <sub>14</sub> H <sub>9</sub> N
	2	119.309°C	303.098°C	16.1541%	17.3091%	
	3	303.098°C	593.121°C	55.0972%	56.1212%	ZnO
Calculated: 76.4437% Final=23.5563% Estimated 77.8428% Final=22.1572%						

### 3.6. Infrared spectra

The infrared spectra of ligand  $H_2L$  and its metal complexes were recorded with  $Cd^{+2}$ ,  $Zn^{+2}$ ,  $Fe^{+3}$ ,  $Mn^{+2}$ , and  $V^{+4}$ , and the data has been organized in Table 5. The ligand showed bands at  $3477$ ,  $3167$ ,  $1546$ - $1600$ , and  $1257$   $cm^{-1}$  that were ascribed to the stretching vibrations of O-H, C-H aromatic, C=C aromatic, and C-O [20]. The infrared spectrum of the ligand showed a medium-intensity stretch band at frequency  $1352$   $cm^{-1}$ , which was attributed to the vibration frequencies of the double bond N=N (Figure 9). The FT-IR spectra of all the prepared compounds showed that the azo-dye ligand was coupled to metal ions through two sites: the oxygen site *via* deprotonation of the phenolic group and the nitrogen site of the azo group [21]. New bands belonging to M-N appeared at  $611$ ,  $617$ ,  $621$ ,  $615$ , and  $619$   $cm^{-1}$  for the  $V^{+4}$ ,  $Mn^{+2}$ ,  $Cd^{+2}$ ,  $Zn^{+2}$ , and  $Fe^{+3}$  complexes, respectively. M-O at  $457$ ,  $462$ ,  $460$ , and  $450$   $cm^{-1}$  for the complexes  $V^{+4}$ ,  $Mn^{+2}$ ,  $Cd^{+2}$ ,  $Zn^{+2}$ , and  $Fe^{+3}$ , respectively. M-Cl at  $385$   $cm^{-1}$  for the  $Fe^{+3}$  complex [22].

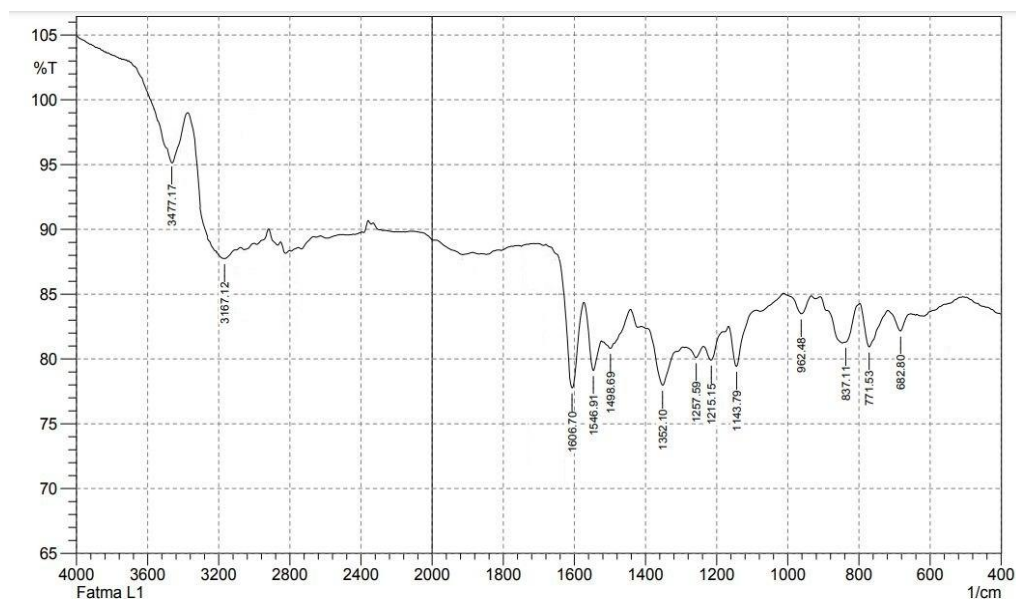


Figure 9: FT-IR spectrum of ligand ( $H_2L$ )

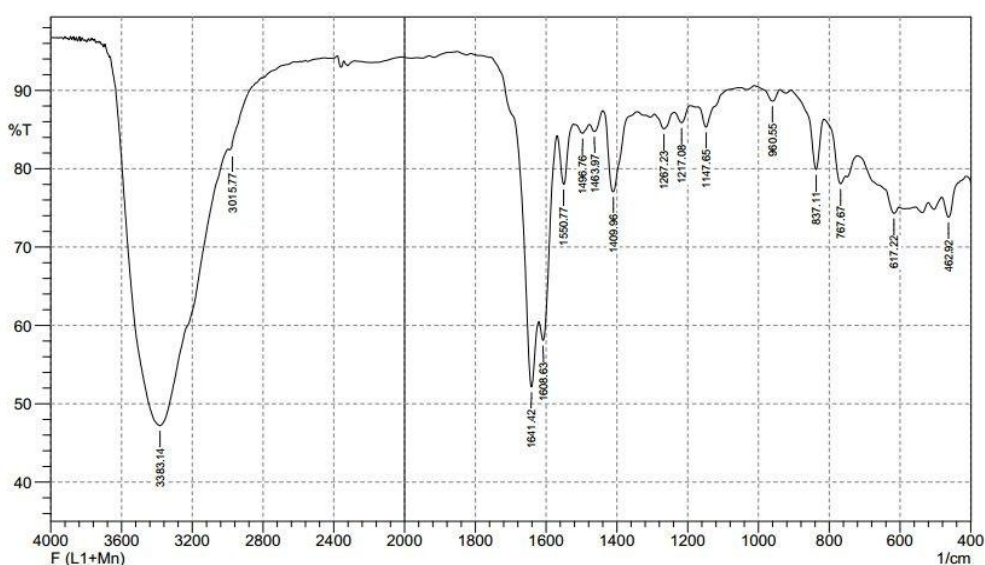


Figure 10 FT-IR spectrum of Mn complex



**Table 5:** The FT-IR spectra bands (cm<sup>-1</sup>) of the ligand and its complexes

Compound	v(H <sub>2</sub> O) aqua	v(C-H) aromatic	v(C-O)	v(N=N)	Other bands
H <sub>2</sub> L	-	3167	1257	1352	
[VO(L)H <sub>2</sub> O]	3410 1643 835	3169	1213	1419	611(V-N) 457(V-O) 979(V=O)
[Mn(L)H <sub>2</sub> O]	3383 1641 837	3015	1217	1409	462(Mn-O) 617(Mn-N)
[Zn(L)H <sub>2</sub> O]	3400 1640 834	3100	1220	1400	615(Zn-N) 460(Zn-O)
[Fe(L)(H <sub>2</sub> O)Cl]	3385 1645 830	3050	1215	1415	619(Fe-N) 450(Fe-O) 385(Fe-Cl)
[Cd(L)H <sub>2</sub> O]	3388 1642 828	3160	1218	1412	621(Cd-N) 458(Cd-O)

**3.7. Investigation of antioxidant activity**

The antioxidant activity of H<sub>2</sub>L and its mineral complexes was measured by ascorbic acid, and the DPPH assay was used to scavenge free radicals. Initially, each sample was diluted with the same volume of methyl alcohol, and then it was mixed with the same volume of a concentrated 0.135 mM DPPH solution. After adding the DPPH solution [23], the samples were kept at room temperature in the dark for 30 minutes. The absorbance of each sample was then determined to be 517 nm. The lower the IC<sub>50</sub> value of the complexes compared to ascorbic acid, the greater their ability to suppress free radicals. As the ligand was the most effective free radical inhibitor, followed by zinc, which has the same value as ascorbic acid, followed by iron, vanadium, cadmium, and manganese [24,25], the values of IC<sub>50</sub> are as follows: H<sub>2</sub>L > D-ascorbic acid > Zn-complex > Fe-complex > V-complex > Cd-complex > Mn-complex (Figure 11).

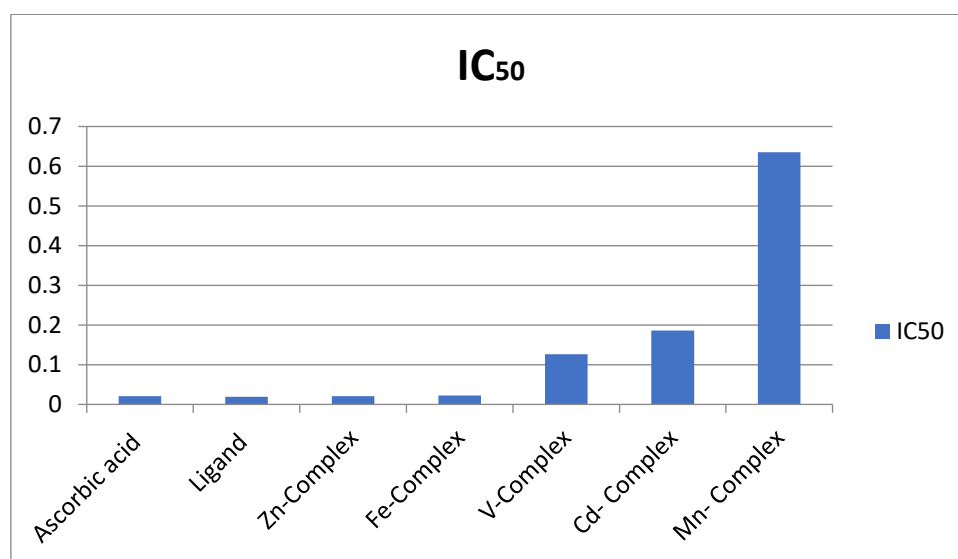


**Figure 11:** Variations of IC<sub>50</sub> values for H<sub>2</sub>L ligand and its complexes

**Table 6:** The antioxidant results (P1%, RSA% and IC<sub>50</sub>) of H<sub>2</sub>L and their metal complexes

Compound	Concentration (mg/mL)	PI (%)	RSA (%)	IC <sub>50</sub> (mg/mL)
Ascorbic acid	0.374	12.29	87.80	0.021
	0.186	36.75	63.25	
	0.03	58.74	41.26	
LigandH <sub>2</sub> L	0.375	18.37	81.63	0.019
	0.186	42.18	57.82	
	0.093	64.17	35.83	
	0.046	77.91	22.09	
Zn- complex	0.113	20.14	79.86	0.021
	0.057	43.95	56.05	
	0.028	65.94	34.06	
	0.014	79.68	20.32	
Fe-complex	0.374	15.27	85.19	0.022
	0.186	39.08	62.07	
	0.093	61.07	40.74	
	0.046	74.81	27.41	
V-complex	0.374	42.86	57.14	0.126
	0.186	46.72	53.28	
	0.093	60.48	39.52	
	0.046	69.36	30.64	
Cd- complex	0.113	67.48	32.52	0.186
	0.057	82.38	17.62	
	0.028	97.28	2.72	
	0.014	99.14	0.86	
Mn-Complex	2.326	68.49	31.51	0.635
	1.285	87.54	12.46	
	0.764	91.98	8.02	
	0.503	96.14	3.86	

#### 4. Conclusion

A novel azo ligand was prepared *via* the reaction of the diazonium salt of 3-aminophenol with 2-hydroxyquinoline. This ligand was then employed to access new complexes with different metals. These complexes were identified using a number of analytical techniques, such as elemental microanalysis, metal chloride-containing, electrical conductivity measurement, magnetic susceptibility, <sup>1</sup>H and <sup>13</sup>C-NMR, FT-IR, and UV-Vis spectroscopy. Calculations of the thermodynamic parameters  $\Delta H$ ,  $\Delta S$ , and  $\Delta G$  were made using the DCS curve, and the atomic N, O, and O tridentate coordination sites in the ligand were identified by comparing their FT-IR spectra to those of the metal complexes. The M:L ratio in every compound was 1:1. The dye used the complexes prepared from it to determine their ability to inhibit free radicals by measuring their ability as antioxidants using DPPH as a free radical and D-ascorbic acid as a standard substance and determining the value of IC<sub>50</sub>. The ligand exhibited a significant capacity to suppress free radicals, and its ability to inhibit the complexes varied depending on the IC<sub>50</sub> value. The results are as follows: H<sub>2</sub>L > D-ascorbic acid > Zn-complex > Fe-complex > V-complex > Cd-complex > Mn-complex.

#### References

- [1] I. H. Ibraheem, N. S. Mubder, M. M. Abdullah, and H. Al-Neshmi, "Synthesis, characterization and bioactivity Study from azo-ligand derived from methyl-2-amino benzoate with some metal ions", *Baghdad Science Journal*, vol. 20, no. 1, pp. 0114-0114, 2023.
- [2] N. Nagasundaram, C. Govindhan, S. Sumitha, N. Sedhu, K. Raguvaran, S. Santhosh, and A. Lalitha, "Synthesis, characterization and biological evaluation of novel azo fused 2,3-dihydro-1H-perimidine derivatives: In vitro antibacterial, antibiofilm, anti-quorum sensing, DFT, in silico ADME and Molecular docking studies", *Journal of Molecular Structure*, vol. 1248, article no. 131437, 2022.

- [3] M.Lashanizadegan, H. A.Ashari, M.Sarkheil, M.Anafcheh, and S.Jahangiry, New Cu(II), Co(II) and Ni(II) azo-Schiff base complexes: Synthesis, characterization, catalytic oxidation of alkenes and DFT study", *Polyhedron*, vol. 200, article no.115148,2021.
- [4] J.Keshavayya, I.Pushpavathi, C. T.Keerthikumar, M. R.Maliyappa, and B. N.Ravi,"Synthesis, characterization, computational and biological studies of nitrothiazole incorporated heterocyclic azo dyes", *Structural Chemistry*,vol.31,no.4,pp.1317-1329, 2020.
- [5] C. Keshava, S. Nicolai, S.V. Vulimiri, A. Cruz, N. Ghoreishi, S. Knueppel, A. Lenzner, P. Tarnow, J. T. Vanselow, B. Schulz, A. Persad, N. Baker, K.A. Thayer, A. J. Williams and R. Pirow, " Application of systematic evidence mapping to identify available data on the potential human health hazards of selected market- relevant azo dyes", *Environment International*, vol.176, article no.107952, pp. 1-12, 2023.
- [6] H. A. K. Kyhoiesh and K. J.Al-Adilee, "Synthesis, spectral characterization, antimicrobial evaluation studies and cytotoxic activity of some transition metal complexes with tridentate (N,N,O) donor azo dye ligand", *Results in Chemistry*,vol. 3,article no. 100245,2021.
- [7] H. S.Mandour, S. A.Abouel-Enein, R. M.Morsi, and L. A.Khorshed," Azo ligand as new corrosion inhibitor for copper metal: Spectral, thermal studies and electrical conductivity of its novel transition metal complexes",*Journal of Molecular Structure*,vol.1225,article no. 129159,2021.
- [8] V. T. Suleman, A. A. S. Al-Hamdani, S. D. Ahmed, V. Y. Jirjees, M. E. Khan, A. Dib, W. Al Zoubi, and Y. G. Ko, "Phosphorus Schiff base ligand and its complexes: Experimental and theoretical investigations",*Applied Organometallic Chemistry*, vol. 34 no. 4, pp. 1-16, 2020.
- [9] G. G. Mohamd, W. H. Mahmoud and A. M. Refaat, "Nano-Azo Ligand and Its Superhydrophobic Complexes: Synthesis, Characterization, DFT, Contact Angle, Molecular Docking, and Antimicrobial Studies," *Journal of Chemistry*, vol. 2020, pp. 1-9, 2020
- [10] S. Benkhaya, S. Mrabet and A Elharfi, " Classifications, properties, recent synthesis and applications of azo dyes", *Heliyon*, vol. 6, article no.e03271, pp.1-26, 2020
- [11] W. Al Zoubi, A. A. S. Al-Hamdani, S. D. Ahmed, H. M. Basheer, R. S. Al-Luhaibi, A. Dib, and Y. G. Ko, "Synthesis, characterization, and antioxidant activities of imine compounds", *Journal of Physical Organic Chemistry*, vol. 32, no. 3, article no. e3916, 2018.
- [12] S. M. Mahdi and A. K. Ismail, "Preparation and Identification of new azo-schiff base ligand (NASAR) and its divalent transition metal Complexes," *Journal of Pharmaceutical Sciences and Research*, vol. 10, no. 9, pp. 2175-2178, 2018.
- [13] K. Mezgebe and E. Mulugeta, "Synthesis and pharmacological activities of azo dye derivatives incorporating heterocyclic scaffolds:a review", *Royal Society of Chemistry*, vol. 12, pp. 25932-25946, 2022.
- [14] N. Sher, N. Fatima, Sh. Perveen, F. A. Siddiqui and A. W. Sial, " Pregabalin and Tranexamic Acid Evaluation by Two Simple and Sensitive Spectrophotometric Methods," *International Journal of Analytical Chemistry*, vol. 2015, no. 24141, pp. 1- 7, 2015.
- [15] A. B. P. Lever, *Inorganic Electronic Spectroscopy*, Elsevier Publishing Company: Amsterdam,London, 1968, p. 121, 6<sup>th</sup> Edition.
- [16] A. G. Prashantha, J. Keshavavayya and R. A. S. Ali, "Synthesis, spectral characterization and biological applications of novel 3-[(4,6-dihydroxy pyrimidin-5-yl) diazenyl]-4-methylbenzoic acid azo dye and their derivatives" , *Results in chemistry*, vol. 3, article no. 100110, pp.1-11, 2021.
- [17] M. Q. Abdulridha and A. A. S. Al-Hamdani, "Synthesis, characterization of new metal complexes of Co(II), Cu(II), Cd(II), and Ru(III) from azo ligand 5-((2-(1H-indol-2-yl)ethyl)diazinyl)-2-amino phenol, thermal and antioxidant studies", *Baghdad Science Journal*, vol. 20, no.5, pp.1964-1975, 2023.
- [18] A.A.S Al-Hamdani, A. M Al-Alwany, T.A. Mseer, A. M. Fadhel, and A. F. Al- Khafaji, "Synthesis, characterization, spectroscopic, thermal and biological studies for new complexes with N1, N2-bis (3-hydroxyphenyl)oxalamide", *Egyptian Journal of Chemistry*, vol. 66, no.4, pp. 223-235, 2022.
- [19] N. M. Mallikarjuna and J. Keshavayya, " Synthesis, spectroscopic characterization and pharmacological studies on novel sulfamethaxazole based azo dye" , *Journal of King Saud University- Science*, vol. 32, pp. 251-259, 2020.
- [20] R. K. H. Al-Daffaay, "Preparation, spectroscopic characterization of transition metal complexes with Schiff base 2-[1-(1H-indol-3-yl)ethylimino)methyl]naphthalene-1-ol", *Baghdad Science Journal*, vol. 20 no. 7, pp. 1036-1044, 2022.

- [21] K. Nakamoto, *Infrared and Raman Spectra of Inorganic and Coordination Compounds*, Wiley-Interscience: New York. 1997.
- [22] R. M. Silverstein, G. C. Bassler and T. C. Morrill, *Spectroscopic Identification of Organic Compounds*. Wiley: New York, 1981, edn4
- [23] K. J. Al-Adilee, H. A. K. Kyhoiesh and A. M. Taher, " Synthesis, characterization, biological studies, molecular docking and theoretical calculation of some transition metal complexes with new azo dye 2-[2-(6-methoxybenzothiazolyl)azo]-3-methyl-4-nitrophenol", *Results in Chemistry*, vol. 4, article no. 100500, pp.1-16, 2022.
- [24] S. Slassi, A. Fix-Tailler, G. Larcher, A. Amine and A. El-Ghayoury, " Imidazole and Azo-Based Schiff Bases Ligands as Highly Active Antifungal and Antioxidant Components," *Heteroatom Chemistry*, vol. 2019, pp. 1-8, 2019.
- [25] I. A. Hussein, "Synthesis, characterization and antioxidant activity of new azo ligand and some metal complexes of tryptamine derivatives", *Baghdad Science Journal*, vol. 20, no.3 pp. 1046-1046,2023.